J. Agric. Sci. Technol. (2006) Vol. 8: 61-76

A Model for Stability Analysis of a Multi-Layered River Bank (SAMLR)

E. Amiri-Tokaldany[1*] and S. E. Darby[2]

ABSTRACT

River bank erosion can result in considerable riparian land loss and the delivery of large volumes of sediment to reaches downstream. Consequently, the ability to predict the stability and failure geometry of eroding river banks is an important prerequisite for estimating the rate of bank erosion and sediment yield associated with bank erosion. In this paper a new model capable of analyzing the stability of layered river banks is introduced. The new model takes into consideration the effects of positive pore water pressure in the saturated portion, and negative pore water pressure in the unsaturated portion, of the bank. Also, the role of hydrostatic confining pressure due to the water level in the river and the effects of the water in tension crack on stability analysis is accounted for. Unlike many previous analyses, the failure plane is not constrained to pass through the toe of the bank. However, it considers only planar-type failure mechanism. Finally the bank profile geometry is not restricted to a special case. The new model has been tested using field data sets from a site on the Sieve River in Italy and a site on Goodwin Creek in Mississippi. The results show some agreement between the predicted and observed values of bank stability.

Keywords: Bank erosion, Bank stability, Failure plane angle, Layered banks, Negative pore pressure, Planar failure, Tension crack.

INTRODUCTION

Riverbank erosion and associated sedimentation and land loss are river engineering and water resource management problems of global significance. In the United States alone, an estimated 142,000 miles (227,000 km) of stream bank are in need of erosion protection, with the cost of protecting US stream banks in 1981 about US $1 billion (US Army Corps of Engineers, 1983). To promote the effective management of rivers subject to bank erosion, models are needed that can provide reliable predictions of the effects of changes in river morphology or bank material characteristics, so that undesirable impacts of channel changes can be avoided.

A wide range of individual processes can contribute to riverbank erosion (Thorne, 1982; American Society of Civil Engineers Task Committee, 1998). These include a wide range of processes of sub-aerial and sub-aqueous weathering, direct removal of bank materials by the shearing action of water in the channels, as well as mass-wasting of banks under the influence of gravity. Of these processes, the erosion of bank material through mass-wasting is probably the most serious river bank erosion from the perspective of water resources management. This is because mass-wasting involves rapid channel widening and the delivery of large volumes of sediment to the channel. Moreover, extensive mass-wasting is usually an indicator of catchment-wide river channel instabil-

[1] Department of Irrigation and Reclamation Engineering, Faculty of Agriculture, University of Tehran, Karaj, Islamic Republic of Iran.
[2] Department of Geography, Southampton University, Southampton, UK. e-mail: S.e.Darby@soton.ac.uk
[*]Corresponding author , e-mail: amiri@ut.ac.ir

[DOR: 20.1001.1.16807073.2006.8.1.6.4]

ity associated with incision of the river bed (Darby and Simon, 1999).

Given the significance of bank erosion through mass failure, it is not surprising that a number of attempts to predict land loss and bank sediment yield associated with riverbank failure (Osman and Thorne, 1988; Lohnes, 1991; Thorne and Abt, 1993) have been made. These approaches are all based on estimating the failure geometry of cohesive banks that become unstable following bed degradation and/or direct fluvial shear erosion. Failure along an approximately planar failure surface takes place when erosion of the bank and the channel bed adjacent to the bank increase the height and steepness of the bank to the point that it reaches a condition of incipient failure. In addition to the influence of river bed erosion, bank failure can also be triggered by changes in the geotechnical characteristics of the bank materials. Examples include loss of cohesion by frost weathering (Lawler, 1986), or occurrence of positive pore pressures following rapid drawdown. The development of tension cracking is also important in promoting bank failures of this type (Darby and Thorne, 1994; 1997). The mechanism of failure depends on the engineering properties of the soil and the geometry of the bank at the point of collapse (Thorne and Abt, 1993).

While the development of riverbank failure analyses has been common, most existing models have a number of technical and conceptual shortcomings. In the past, most analyses of the stability of steep, cohesive, eroding banks which fail along planar surfaces have been based on estimating the resultant of both driving and resisting forces acting on incipient failure blocks using a relatively simple, idealized, geometry. Examples of analyses based on geometries of this type include Lohnes and Handy (1968), Thorne *et al.* (1981), Huang (1983) and Simon *et al.* (1991). Such analyses are somewhat limited when they are applied under conditions encountered in the field (Darby and Thorne, 1996a; Millar and Quick, 1997), for the following reasons:

-Idealized bank profiles are inadequate to characterize the profile of natural, eroding riverbanks, particularly when a tension crack is present (Osman and Thorne, 1988). Combinations of near-bank bed degradation and bank-toe erosion tend to result in a characteristic bank profile more akin to that shown in Figure 1.

In Figure 1, H is Height of river bank, W.L. is the level of river water surface, R.I. is the elevation of the river bed, BW is the location of the tension crack or the magnitude of the bank retreat, N.G. is the natural ground level, G.W.L. is the level of the

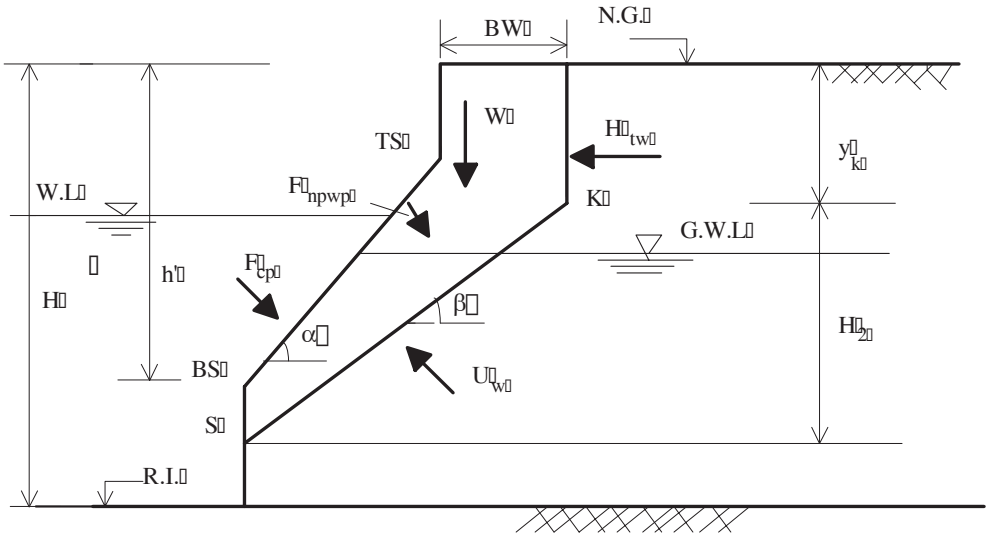

Figure 1. The framework for river bank stability analysis.

[DOR: 20.1001.1.16807073.2006.8.1.6.4]

ground water, α and β are angles of river bank before and after bank failure, respectively, and y_k is the depth of the tension crack. Points TS, BS, S, K, along with heights h' and H_2 are used to define the geometry of the river bank.

-The failure plane is constrained to pass through the toe of the bank. Field observations indicate this is sometimes unrealistic (Simon *et al*., 1991).

-The effects of soil pore water pressures and the hydrostatic confining pressure of water in the channel are usually either ignored, or characterized by a simplified pore pressure ratio term (Simon *et al*., 1991).

-Application of the planar failure analysis is restricted to very steep banks (Taylor, 1948; Millar and Quick, 1997).

-Most existing models assume that the bank is composed of homogenous bank materials, such that the influence of discrete stratigraphic horizons within the vertical structure of the bank are not accounted for.

Some of the above limitations have individually, or in combination, been addressed in more sophisticated analyses (Darby and Thorne, 1996b). Osman and Thorne (1988) based their stability analysis on the bank profile shown in Figure 1, but they still assumed that the failure plane passes through the toe of the bank, and pore water and hydrostatic confining pressure effects were neglected. On the other hand, pore water and hydrostatic confining pressure effects were included in an analysis developed by Simon *et al*. (1991), but in which the idealized bank profile of Figure 1 was retained. More recently Rinaldi and Casagli (1999) and Simon *et al.* (2000) have developed analyses focusing attention on the effects of negative pore water pressures in the unsaturated portion of the bank, the stabilizing effects of the hydrostatic confining pressure, and the destabilizing effects of positive pore water pressures in the saturated part of the bank. These analyses provide realistic representations of the effects of pore water pressures in the saturated and unsaturated parts of the bank profile, which is an important advance, but they still retain a very simplified bank profile.

To address some of these limitations, a new analysis of bank stability is presented in this paper. The new model accounts for the geotechnical characteristics of the bank materials; i.e. soil cohesion, friction angle, saturated and unsaturated specific weight, the shape of the bank profile, and the role of hydrostatic and pore water pressures (both positive and negative). The key advance of the new model is its ability to take into account the effects of multiple layers of soil, each with different physical properties, within the sedimentary structure of the bank. Finally, the new model is tested using data from two discrete study sites and predictions of factor of safety are found to be in very close agreement with the observed values.

MATERIALS AND METHODS

In Figure 1, the framework for analysis of the stability of a natural river bank, together with the forces acting on the incipient failure block, are illustrated. Bank stability may be modelled using the factor of safety concept:

$$FS = \frac{FR}{FM} \qquad (1$$

where FS is the factor of safety against block sliding, and FR and FM are the resultant resisting and motivating forces acting on a unit width of the failure block, respectively. Hence, bank failure is predicted to occur once the ratio of resisting and motivating forces falls below unity. The resultant motivating force acting on a unit width of the failure block is given by:

$$FM = W \sin\beta - F_{cp} \sin i + H_{tw} \cos\beta \qquad (2$$

(Figure 5), where β is the failure plane angle (degrees), i is the angle between the direction of the resultant of the hydrostatic confining pressure and a normal to the failure plane (degrees), W is the weight of a unit width of the failure block (N/m), F_{cp} is the hydrostatic confining pressure acting on a unit width of the failure block (N/m), and

[DOR: 20.1001.1.16807073.2006.8.1.6.4]

H_{tw} is the hydrostatic force exerted by any water present in the tension crack on a unit width of the failure block (N/m). The resultant resisting force acting on the failure block is given by:

$$FR = \overline{c'}L + \varphi ta\phi^b + (W\cos\beta + F_{cp}\cos i - U_w - H_{tw}\sin\beta) \times \tan\overline{\phi'} \quad (3$$

where $\overline{c'}$ is the weighted average of the cohesion force acting on the surface of failure plane (N/m), L is the length of the failure plane (m), φ is the negative pore water pressure (N/m), ϕ^b is the angle expressing the strength increase rate relating to the negative pore water pressure, U_w is the uplift force due to any positive pore water pressure acting on a unit width of the failure block (N/m), and $\overline{\phi'}$ is the weighted average of the friction angle value in each soil layer (degree). The model does not directly take into account the effect of shear stress exerted by water flowing in the channel on the river bank materials. This is because in most channels, the magnitude of shear stress relative to the hydrostatic force is negligible. As a result, this limitation does not affect the bank stability analysis. The long-term effects of shear stress on the stability of the slope is, however, indirectly accounted for by changing the bank profile as a result of fluvial erosion. The next step is to introduce the method by which the above parameters are calculated.

Calculation of the Weight of the Failure Block

In the stability analysis of a multi-layered river bank, the weight of the failure block is equated to the sum of the weight of each layer so that:

$$W(k) = A(k) \times \gamma_{so}(k) \quad (4$$

$$W = \sum_{k=1}^{n} W(k) \quad (5$$

where $A(k)$ is the area projected by layer k (m^2), $\gamma_{so}(k)$ is the specific weight of soil layer k (N/m^3), $W(k)$ is the weight of layer k (N/m), and n is the total number of soil layers present within the bank.

Calculation of Positive and Negative Pore Water Pressures

Water in the pores of a saturated soil has a pressure which (on the condition of hydrostatic pressure distribution) is conveniently represented by the height of water, h_w, within the pores. By assuming hydrostatic pressure distribution, the amount of pore water pressure at a point such as A is equal to:

$$P_A = \gamma_w \times h_w \quad (6$$

where P_A is the magnitude of the positive pore water pressure (N/m^2), γ_w is the specific weight of water (N/m^3), and h_w is the height of the water table above the point A (m). In the region between the water table and ground surface levels, there may be three sub-regions: a dry sub-region, an unsaturated or partially saturated zone, and a saturated zone.

In the dry sub-region, which is normally located near the ground level, the pore pressure is zero. It is noteworthy that entirely dry soils are actually relatively rare but can be found on beaches above the high-tide mark (Atkinson, 1993). Therefore, even under "dry" conditions, most soils have a finite amount of water retained that is related to the physical characteristics of the soil. This means that the amount of water content, and consequently, the negative pore water pressure in this zone are constant.

Immediately above the water table, the soil remains saturated due to capillary rise in the pore spaces. In this sub-region, the pore water pressure is negative and, at point A, is given by:

$$\varphi_A = -\gamma_w \times h_w \quad (7$$

where φ_A is the negative pore water pressure (for positive values of h_A) or matric suction (for negative values of h_A) at point A

[DOR: 20.1001.1.16807073.2006.8.1.6.4]

(N/m^2), and h_A is the height of point *A* (m) above the water table. The extent of the saturated sub-region immediately above the water table depends inversely on the size of grains, or more particularly on the size of the pore spaces. Hence, the greater the magnitude of the grains and pores, the smaller the extent of the saturated soil (Atkinson, 1993).

Between the dry and saturated sub-regions, there is a zone of unsaturated or partially saturated soil which contains soil grains, water and gas, usually air or water vapour. The degree of saturation in this zone depends on the size and structural characteristics of the soil. In this area, the pressure of the pore water and pore gas are different and pore water suction may increase or decrease. This case is found very near the ground surface, in compacted soils, and in hot dry climates. From the point of view of bank stability, the presence of positive pore water pressure decreases the resisting force due to the vertical component of weight of the overlying bank material, thereby causing a reduction in bank stability. In contrast, negative pore water pressure increases the apparent shear strength of the bank material and helps to stabilize the bank (Rinaldi and Casagli, 1999).

On the basis of the above, an example of the way in which positive pore water pressure is calculated is introduced. As is shown in Figure 2, in the case that the water level in the river is below point S, the pore water pressure at points A,B,C,D and S are equal to $h_1\gamma_w$, $h_2\gamma_w$, $h_3\gamma_w$, $h_4\gamma_w$, and 0.0 respectively. It can be seen that the resultant pore water forces acting on the failure plane are equal to the area of polygon ABCDS4321. Moreover, a case in which the water level in the river is above point S is given in Figure 3. It should be noted that to obtain the amount of positive pore water pressure it is assumed that the phreatic line is horizontal. This is recognized as a limitation, but it is necessary in order to simplify the analysis.

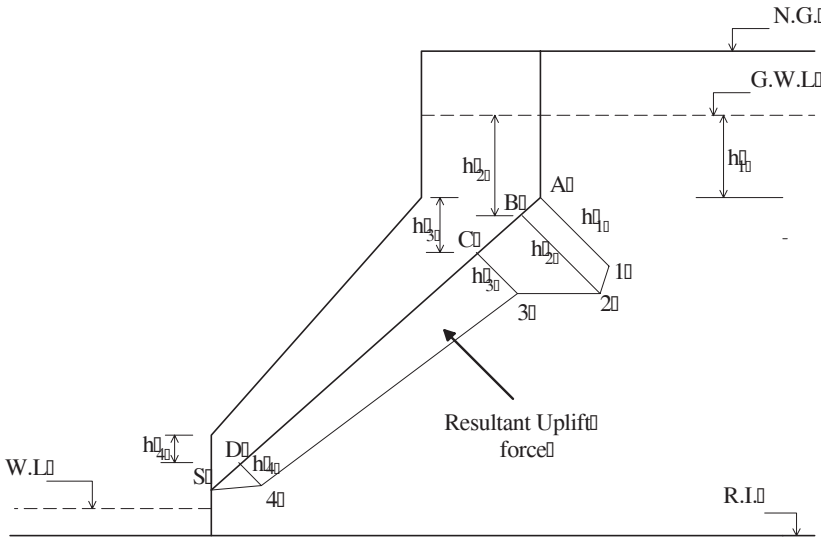

Figure 2. Computation of uplift force (W.L. is below point S).

Likewise, the calculation of negative pore water pressure in the saturated zone above the water table is similar to the method used to calculate the positive pore water pressure, albeit with a negative sign. In this regard, it is necessary to determine the height of capillary rise. Generally, for a liquid inside a tube, the height of capillary rise (h_{CR}) is equal to:

[DOR: 20.1001.1.16807073.2006.8.1.6.4]

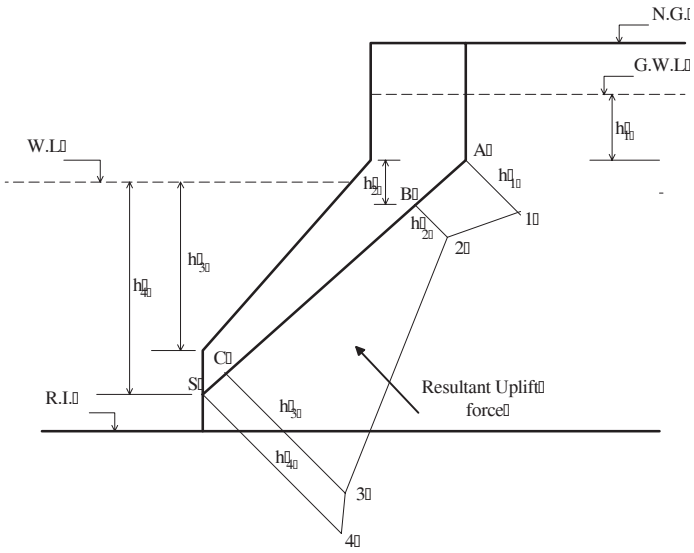

Figure 3. Computation of uplift force (W.L. is above point S).

$$h_{CR} = \frac{4\sigma \cos\theta}{\gamma_w d} \qquad (8$$

where θ is the angle of contact between liquid and solid (degrees), d is the average diameter of the tube (m), and σ is the magnitude of the surface tension (N/m) of liquid, which varies with temperature. For instance, for water in a glass tube at 20° C, the magnitude of σ is equal to 0.0727 (N/m) (Douglas *et al.*, 1995), while the magnitude of θ is nearly equal to zero. To extend equation (8) for application to natural soils, however, it must be realized that the capillary tubes formed in soils have variable cross sections. This results in a variable degree of saturation with height through the soil column. A commonly used approximation for the effective pore diameter is (Bowles, 1979):

$$d \cong 0.2 D_{10} \qquad (9$$

where D_{10} is the grain size for which 10% of the particle size distribution is finer. For instance, in clayey soils where D_{10} may be on the order of 0.0015 mm, pore diameter is about 0.0003 mm. Therefore, the corresponding height of capillary rise in clayey soils is about 10 meters. However, Due to evaporation, which results in water being removed as fast as it is pulled up to a higher elevation, the theoretical height of capillary rise is actually reduced to about 1 to 2 meters under realistic conditions.

After determining the height of capillary rise, it may be assumed that the pressure at any point like *A* in the capillary tube above the free water surface will be negative with respect to the atmospheric pressure, the magnitude of which is given by $-h_A \gamma_w$.

Unfortunately, there is at present no simple and satisfactory theory to estimate the amount of negative pore water pressure in the unsaturated region. For an unsaturated soil, Fredlund *et al.* (1978) proposed that the shear strength can be expressed as following form:

$$\tau_{ss} = c' + (\sigma - u_w)\tan\phi' + \varphi \tan\phi^b \qquad (10$$

where τ_{ss} is the shear strength, and φ is matric suction (u_a-u_w).

Many laboratory studies have developed formulae to compute the value of matric suction in equation (10). For instance, Visser (cited in Hillel, 1971) reported:

$$\varphi = a(P_s - \theta_w)\left(\frac{b}{\theta_w^c}\right) \qquad (11$$

[DOR: 20.1001.1.16807073.2006.8.1.6.4]

where P_s is the soil porosity, θ_w is volumetric wetness, and *a*, *b*, and *c* are empirical coefficients that vary between 0.0-3.0, 0.0-10.0, and 0.4-0.6, respectively.

Alternatively, Gardner *et al*. (cited in Hillel, 1971) suggested:

$$\varphi = a\theta_w^{\,b} \qquad (12$$

where *b* is equal to 4.3 for a fine sandy soil, but *a* has the same values mentioned before.

Regarding the determination of ϕ^b, Fredlund and Rahardjo (1993) reported that the value of ϕ^b varies with matric suction from its maximum at saturation $(\phi^b = \phi')$, and then decreases with increasing matric suction until ϕ^b reaches a steady value. Rinaldi and Casagli (1999) performed Borehole Shear Tests (BST) at a study site located on the Sieve River in Tuscany, Italy. Rinaldi and Casagli (1999) reported a large scatter of ϕ^b values ranging from 10 to 26 degrees, with a mean value of 16 degrees. Simon *et al*. (1999), working on Goodwin Creek in Mississippi, USA, reported the values of 10.4, 17.5, and 17.5 degrees for discrete layers comprising the upper, middle, and lower parts of the bank, respectively. The above values are the only data currently available to describe the value of ϕ^b in natural river banks. Therefore, in cases where no data are available, a ϕ^b value between 10-26 degrees is used in the present model.

In Figure, 4 an example of computing negative pore water pressure by using field data is shown. It is assumed that each measured point value is representative of the total thickness of the relevant soil layer. The area of the relevant polygon times the specific weight of water gives the magnitude of force due to negative pore water pressure. It should be noted that the pressure heights at each point of the sliding length (shown in Figure 4) is the product of the matric suction (φ) and $\tan\phi^b$.

Calculation of Hydrostatic Confining Pressure

To obtain the value of hydrostatic confining force exerted on the failure plane, the parameters of interest are the magnitude of the resultant confining pressure, F_{cp}, and the angles, ω, and *i*, at which the resultant is directed through the bank surface and failure plane, respectively (Figure 5). The resultant hydrostatic confining force acting on an inclined river bank consists of the forces acting horizontally and vertically on the bank surface. The vertical force (F_y) is due to the

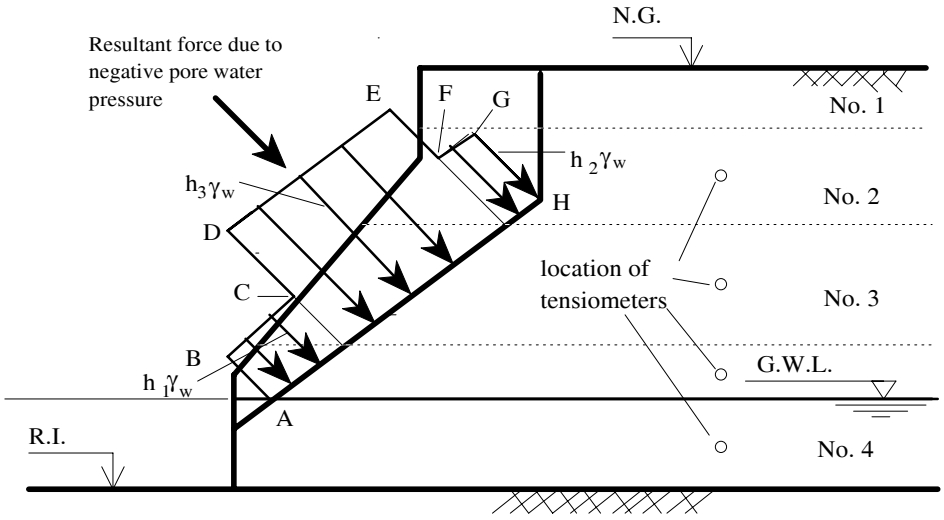

Figure 4. Computation of force due to negative pore water pressure using the values of matric suction measured by tensiometers.

[DOR: 20.1001.1.16807073.2006.8.1.6.4]

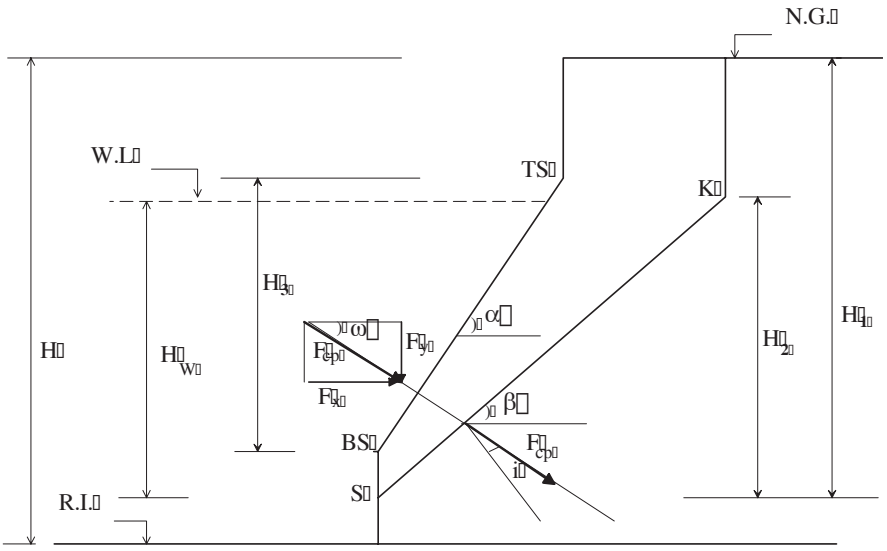

Figure 5. Parameters of hydrostatic confining force and failure plane angle using the Stability approach.

weight of water on the slopped bank face. The horizontal force is due to hydrostatic pressure and is equal to (Douglas *et al.*, 1995):

$$F_x = 0.5 \times H_w^2 \times \gamma_w \quad (13$$

where H_w is the depth of water in the river over point S. The resultant hydrostatic confining force (F_{cp}), and the angle at which the resultant is directed through the bank surface (ω) are determined using the following equations (e.g. Douglas *et al.*, 1995):

$$F_{cp} = \sqrt{F_x^2 + F_y^2} \quad (14$$

$$\omega = \tan^{-1} \frac{F_y}{F_x} \quad (15$$

$$i = 90 - (\beta + \omega) \quad (16$$

where i is the angle between direction of the confining pressure and a normal to the failure plane.

Calculation of Hydrostatic Pressure Due to Water in Tension Crack

Notably, the depth of the tension crack, and its location, affects significantly the geometric specifications of a failed block, e.g. the failure plane angle. It has been reported that tension cracks develop at the instant of failure (Taylor, 1948; Terzhagi and Peck, 1967). In other words, at the time of failure, a block of soil accelerates down the inclined failure plane (Darby and Thorn, 1994). The lateral component of this acceleration can be assumed to generate the lateral tensile stress and consequently, cause the formation of a tension crack. In cases where the tension crack is filled with water (e.g. through rainfall, runoff, or if the ground water level is high), the water in the crack exerts a hydrostatic force (H_{tw}) on the failure block given by:

$$H_{tw} = 0.5 \times h_1^2 \times \gamma_w \quad (17$$

where h_1 is the depth of water in the tension crack (Figure 2). In case that the ground water table is below the point K, this force is equal to zero.

Determination of Failure Plane Angle

The failure plane angle, β, is one of the most important parameters in assessing river bank stability. Taylor (1948), Spangler and Handy (1982), and Osman and Thorne

[DOR: 20.1001.1.16807073.2006.8.1.6.4]

(1988) stated that, under critical conditions, the failure plane angle corresponds to the angle at which the cohesion, c, is fully developed, as expressed by:

$$\frac{\partial c}{\partial \beta} = 0.0 \quad (18$$

By neglecting the effects of positive and negative pore water pressures, hydrostatic confining pressure, and hydrostatic pressure due to water in any tension crack in equations (1), (2), and (3), Osman and Thorne (1988) developed the following equation to predict β:

$$\beta = \frac{1}{2}\left(\tan^{-1}\left[\left(\frac{H}{h'} \right)^2 (1-K_r^2) \tan\alpha \right] + \phi' \right) \quad (19$$

where H and h', are the parameters that are shown in Figure 1, and K_r is the ratio of the depth of tension crack; i.e. y_k to the total height of the bank, H. A comparison of failure plane angles predicted using equation (19) with failure plane angles measured at 51 sites shows that the above equation has a tendency to under-predict the failure plane angle (Darby and Thorne, 1996b). Darby and Thorne (1996b) also reported there was greater disagreement between failure plane angles predicted by Lohnes-Handy's analysis (Lohnes and Handy, 1968) and Huang's analysis (Huang, 1983) with failure plane angles measured at these 51 sites. With the aim of addressing this limitation, Darby and Thorne (1996b) proposed a method for computing β on the basis of their stability equations. Unlike the Osman-Thorne method, however, it seems that this method has a tendency both to over-predict and under-predict the failure plane angle (Darby and Thorne, 1996b). Finally, Rinaldi and Casagli (1999) have used the equation introduced by Hoek and Bray (1981) in which:

$$\beta = 0.5 \times (\alpha + \phi') \quad (20$$

It may be seen that the above equation is a special case of the Osman-Thorne equation when $H = h'$ and $K_r = 0.0$.

In the present model, initially, three methods for computing the failure plane angle have been used. These are as follows:

-The Osman-Thorne method (equation (19)).

-The Modified Darby-Thorne method.

-The Stability approach.

Due to the simplicity of the Osman-Thorne equation, there is no further need to explain it. But, in the case of the Darby-Thorne method, since they did not take into consideration the effects of negative pore water pressure and/or the hydrostatic force applied by water in a tension crack, it is necessary to modify their method. The "Stability approach" is a different numerical solution of the bank stability analysis for predicting failure plane angle. In the following sections, the criteria for the second and the third methods for computing β are explained.

Modified Darby-Thorne Method

Regarding Darby and Thorne's (1996b) method for estimating failure plane angle, and by rearranging equations (1), (2) and (3), it is found that:

$$c' = \frac{W \sin^2\beta - F_{cp}\cos(\beta+\omega)\sin\beta + H_{tw}\cos\beta\sin\beta}{H_2} + \frac{U_w \tan\phi \sin\beta - F_{npwp}\sin\beta - W\cos\beta\sin\beta\tan\phi}{H_2} + \frac{H_{tw}\sin^2\beta\tan\phi - F_{cp}\sin(\omega+\beta)\tan\phi\sin\beta}{H_2} \quad (21$$

in which H_2 is the difference between the elevation of points K and S. Hence:

$$c' = f(\beta) \quad (22$$

With respect to equation (18) it is seen that:

$$\frac{\partial f(\beta)}{\partial \beta} = 0.0 \quad (23$$

After differentiating the above equation and equating the result to zero using the *Newton-Raphson* iteration solution, the value of β can be estimated.

Similar to the Darby-Thorne method, in this method an initial estimate of the failure plane angle is made using equation (20). Convergence is obtained if the error tolerance between two successive solutions is

[DOR: 20.1001.1.16807073.2006.8.1.6.4]

less than 0.01. In some instances, due to certain combinations of W, F_{npwp}, U_w and H_{tw}, convergence does not occur. In these cases, therefore, the model uses equation (20) to estimate the value of failure plane angle.

Stability Approach to Estimate the Failure Plane Angle

Due to the poor predictive ability of existing methods, it is necessary to develop a new approach to achieve a better estimate of failure plane angle. The new approach to predict the angle of bank failure here is similar to the method of the circular surface stability analysis of slopes, wherein a number of different slip circles must be investigated in order to find the one with the lowest factor of safety. Likewise, in the new approach, by considering a number of combinations of the magnitude of the elevation of the toe of the failed bank (point S), and the amount of river bank retreat (BW), the factor of safety for each combination is calculated. It is assumed here that the depth of the tension crack is known and is equal to the difference between the elevation of points N.G. and TS (Figure 1), and that the other geometry characteristics of the bank are constant. For each case once the factor of safety falls below unity, then bank failure takes place and consequently, the failure block angle, β, can be computed as (Figure 5):

$$\beta = \tan^{-1}\left(\frac{H_2}{BW + H_3/\tan\alpha}\right) \qquad (24$$

Furthermore, it is obvious that for any combination of selected values for the bank retreat (BW), and the elevation of point S while the other parameters are constant, there might be a bank failure at a specific time. Therefore, there should be the possibility of a set of river bank failures existing at any study site. To select the relevant time of any bank failure, following Simons and Li (1982), Thorne (1990), Casagli and Rinaldi (1995), Hagerty *et al.* (1995), and Simon and Darby (1999), the bank failure which is closest to the time of the peak flow is recognized as the critical case. This is the basis for the above approach to estimating the failure plane angle, here named the "Stability approach". It should be noted that in developing this approach, it is assumed that within some distance normal to the river bank, the soil materials are homogenous in horizontal extension. From a practical point of view, it is assumed in the model that the elevation of point S in Figure 1 is varied from the elevation of the river bed, i.e. point R.I., to the bottom elevation of the tension crack; i.e. point K. This processes is repeated for each individual value of the bank retreat, so that for each value of the elevation of point S, there may be an individual value of the failure plane angle. However, with respect to the values of α and related β in the 51 study sites used by Darby and Thorne (Darby and Thorne, 1996b), and also with respect to the values of these angles at the Sieve River study site, in the stability approach the value of β is equated to the larger of the following:

$$\beta_{max} = \alpha + 15 \qquad (25$$

$$\beta_{max} = \overline{\phi'} + 15 \qquad (26$$

Limitations of the Model

In so far as the new approach presented here takes into account the effects of a wide range of parameters influencing river bank stability, it is a development in this area of research. However, some limitations remain. First, the present analysis considers only planar-type failure mechanisms. The effects of vegetation have not been considered and, in calculating the pore water pressure, it is assumed that the phreatic surface is parallel to the floodplain surface. The distribution of water pressure in the channel adjacent to the bank is also assumed to be hydrostatic.

Model Testing and Results

In order to assess the predictive ability of the new model, it has been tested using two

[DOR: 20.1001.1.16807073.2006.8.1.6.4]

sets of data which have previously been published. These consist of data from the Sieve River in Italy (Rinaldi and Casagli, 1999), and data from Goodwin Creek in Mississippi (Simon *et al*., 1999). Both rivers have experienced bank retreat that involved mass failure. Brief descriptions of the characteristics of the two streams and their associated data are given here below.

The Sieve River

The Sieve River is a tributary of the Arno, the largest river in Tuscany (Rinaldi and Casagli, 1999). The total length of the river is 58 km. The study site is located some 50 m downstream from the gauging station of Fornacina. The bank here consists of 1.7 m of imbricated gravel with interstitial sand in the lower part, above which there is a 2.9 m thick layer of silt and sand. In this site a series of piezo-tensiometers have been installed in the bank, so that the role of positive and negative pore water pressures in controlling bank stability can be assessed. Figure 6 shows the geometry of the study bank and the location of the tensiometers. The physical properties of the river bank materials at the above study site can be found in relevant paper ([Table 3, Rinaldi and Casagli, 1999)].

During their monitoring study, Rinaldi and Casagli (1999) reported a bank failure with a delay of some hours after the peak flow at around 20:00 on 14 December 1996. They also reported that the mechanism of failure was planar with a tension crack, as illustrated in Figure 6. Simulations were undertaken to attempt to replicate this failure event and thereby test the present model, using the data given in the relevant paper and Figure 6 along with the record of 14 December 1996 (Casagli *et al*., 1999).

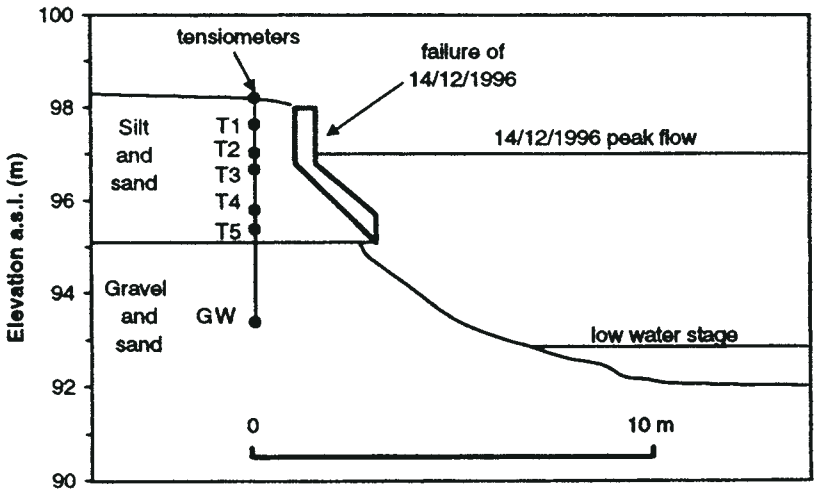

Figure 6. The geometry of the bank at the Sieve River study site (from Casagli *et al.*, 1999).

Regarding the above data, the stability analysis has been performed using each of the three methods for computing the failure plane angle. For all methods, it was assumed that the depth of the tension crack is equal to the difference between the elevation of points N.G. and TS. In Tables 1 and 2 the results for all methods are shown. From Table 1, it is seen that all methods predicted a bank failure on 14/12/96 at nearly the same time. Also, the elevation of point S, i.e. the toe of the failed block in the all methods, is

[DOR: 20.1001.1.16807073.2006.8.1.6.4]

Table 1. Computation of predicted and observed values of time of bank failure and bank failure geometry at the Sieve River study site.

Method	Time of failure	El. S (m)	y_k (m)	β (deg.)	BW (m)
Osman-Thorne	19:56	95.00	1.2	39.6	0.72
Modified Darby-Thorne	19:59	95.00	1.2	38.76	0.79
Stability approach (earliest)	19:51	95.00	1.2	42.7	0.50
Observed values	20:00	95.00	1.2	42.7	0.50

the same. However, there are a few minor differences between the methods regarding the predicted magnitude of the failure plane angle and the amount of bank retreat. The results showed that Osman-Thorne, and Modified Darby-Thorne models predicted a bank failure at 19:55 and 19:59 on 14/12/1996, respectively (Table 1), but the Stability approach predicted more than one bank failure (Table 2). However, from these bank failures, the earliest failure (i.e. the one predicted at 19:51), has been recognized as the critical case.

On the other hand, with respect to the reported values of BW and β, it is observed that the results of the Stability approach are almost the same as the field data. Moreover, it can be seen that one of the bank failures predicted by the Stability approach (predicted at 20:00), is identical to the one predicted by Modified Darby-Thorne method. Since the basic theorems for the Modified Darby-Thorne and the Stability approach are identical, this suggests that the right bank failure predicted by the Stability approach should be identical to the one predicted by the Modified Darby-Thorne method.

Table 2. Bank failure and bank failure geometry predicted by the Stability approach at the Sieve River study site.

Time of failure	El. S (m)	y_k (m)	β (deg.)	BW (m)
19:51	95.00	1.20	42.7	0.50
19:52	95.00	1.20	41.28	0.60
19:55	95.00	1.20	39.93	0.70
19:58	95.00	1.20	45.8	0.30
20:00	95.00	1.20	38.66	0.80

A second attempt to test the model using field data for a discrete event has also been made. In this case, the stability of the river bank at the same site has been studied for the flow of 15/02/97. To do this, it was assumed that the bank profile was changed to a new one following bank failure on 14/12/96. Data for the negative pore water pressure, the fluctuation of both water level in the river and in the ground, provided from Casagli *et al*., (1999, [Figure 6, page 1106]), while the other data were the same as the first case. Agreement between the model predictions and field data is good in that no bank failures are predicted for this event, which is consistent with the fact that none were observed at this time.

Goodwin Creek, Mississippi

Goodwin Creek is a typical incised channel in Northern Mississippi Simon *et al.* (1999). Along this creek, bank materials are composed of three layers: about 2.0 m of moderately cohesive brown, clayey-silt at the top (LH unit), about 1.5 m of blocky-silt of low cohesion and lower permeability in the middle (EH unit), and 2.5 m sand and packed sandy gravel (sand unit) at the toe. Like the Sieve River, the Goodwin Creek study site has been extensively monitored, and time series of cross-sections and pore pressure values, have been collected (see Figure 7 and Simon *et al*. (1999, [Figure 6.6, page 137]).

At this site, continuous measurement of pore water pressure at five depths (30, 148, 200, 270, and 433 cm from the top of the

[DOR: 20.1001.1.16807073.2006.8.1.6.4]

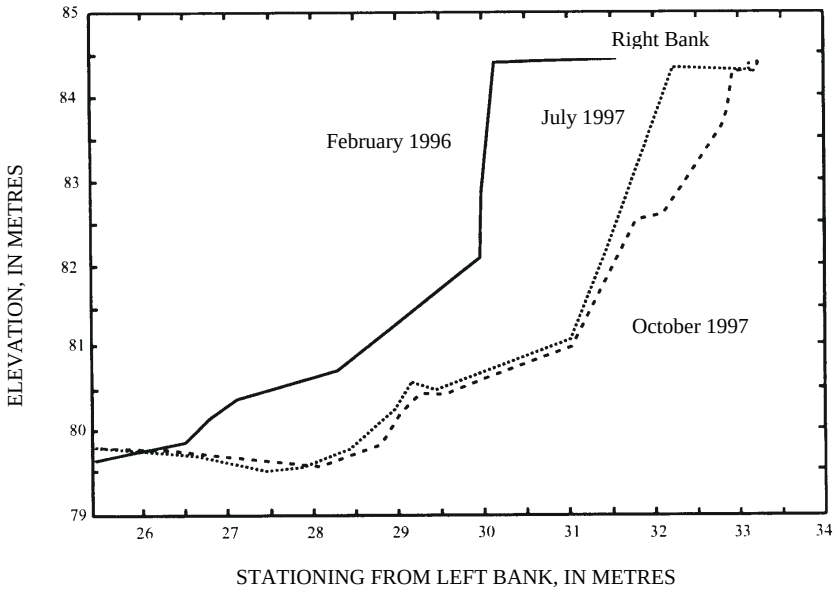

Figure 7. A selected time series cross-section at the Goodwin Creek study site (from Simon *et al.*, 1999).

bank) has been undertaken along a 4.7 m high unstable stream bank since November 1996. Using an Iowa Borehole Shear Tester (Luttenegger and Hallberg, 1981), parameters of apparent or total cohesion (c_a) and effective friction angle (ϕ') were measured in situ. Simon *et al.* (1999) also computed the magnitude of the rate of increase in shear strength due to matric suction (ϕ^b). The geotechnical characteristics of bank materials at Goodwin Creek site are illustrated in Simon *et al*. (1999).

Simon *et al*. (1999) reported that four major failures took place at the Goodwin Creek research site between February and December 1996, resulting in up to 2 m of top bank retreat. Additional failures occurred during September 1997, as well as in January and March 1998. All failures occurred after recession of stormflows. To test the model using data from Goodwin Creek, the first bank failure event in 1996 has been used as the basis for detailed comparison of model predictions versus field data. In this regard, for the analysis of bank stability between February and December 1996, Figure 7 is used as the basis for defining the bank geometry. In addition, the values of matric suction at different depths, together with the stage of water, are used as input data for the model. All data values are derived from the information reported by Simon *et al.* in Simon *et al*. (1999, [Figure 6.5, page 135]). Due to lack of data on the ground water level, it is assumed that the elevation of the ground water level is nearly equal to the elevation of the water in the river but, with a delay.

Using the afore mentioned data, predictions obtained using the above methods are shown on Tables 3 and 4. Table 3 shows that all methods predicted bank failure at the above study sites. Agreement with the available field data is also good (Table 3).

These results confirm the validity of the predictions of bank failure obtained when using the present model. Table 3 shows that there is a close agreement between predictions obtained by the Osman-Thorne and the Modified Darby-Thorne methods on the bank retreat and the failure bank angle. However, both methods predicted the time

[DOR: 20.1001.1.16807073.2006.8.1.6.4]

Table 3. Computation of predicted and observed values of time of bank failure and bank failure geometry at the Goodwin Creek study site.

Method	Time of failure	El. S (m)	y_k (m)	β (deg.)	BW (m)
Osman-Thorne	11:41	79.65	2.29	38.6	1.32
Modified Darby-Thorne	11:47	79.65	2.29	38.0	1.36
Stability approach (earliest)	11:11	79.65	2.29	41.6	1.00
Observed values	11:01	N.A.	N.A.	N.A.	N.A.

of bank failure sometimes (about 40 minutes) after the reported value (11:01). The earliest bank failure predicted by the Stability approach is a little different in terms of the bank retreat and failure bank angle from the other two methods, but it predicted the failure time (11:11) closer to the observed value. Moreover, from Table 4 it can be seen that the fourth bank failure predicted by the Stability approach is very close to the predictions by two other models.

Table 4. Bank failure and bank failure geometry predicted by Stability approach at the Goodwin Creek study site.

Time of failure	El. S (m)	y_k (m)	β (deg.)	BW (m)
11:11	79.65	2.29	41.6	1.00
11:19	79.65	2.29	40.6	1.10
11:28	79.65	2.29	39.57	1.20
11:40	79.65	2.29	38.6	1.30
11:52	79.65	2.29	37.71	1.40

Unfortunately, the geometry of the bank after the first failure is not described by Simon *et al*. (1999). Hence, at present, there is no explicit way to assess the above results or to compare the bank failure geometry predicted by the model with conditions observed in the field at the study site.

CONCLUSION

Riverbank erosion processes are responsible for significant riparian land loss and the delivery of large volumes of sediment, with associated sedimentation hazards, to the downstream reaches of a fluvial system. Hence, the ability to predict the stability and failure geometry of eroding river banks is an important prerequisite for estimating the rate of bank erosion and sediment yield associated with bank erosion. In this study, a physically-based model has been developed to predict the stability of layered river banks that fail along planar failure surfaces. In addition to taking into consideration the effects of positive pore water pressure and the hydrostatic confining pressure, a significant feature of the new model is its ability to consider effects of negative pore water pressure in the unsaturated portion of the bank.

When tested using high-quality field data, the new model has described the behaviour of unstable river banks at both the Sieve River and Goodwin Creek study sites. This supports the view that the present model adequately takes into account the effects of most of the important parameters. On the other hand, the model only considers planar failures. Other failure mechanisms are out of the scope of this research h, which is, however, a limitation of the model. Furthermore, additional research is required to account for the effects of riparian vegetation on bank stability.

REFERENCES

1. American Society of Civil Engineers Task Committee on River Widening, 1998. River Width Adjustment. I: Processes and Mechanisms. *J. Hydr. Engrg, ASCE*, **124**: 881-902.
2. Atkinson, J., 1993. An Introduction to the Mechanics of Soils and Foundations. McGraw-Hill International (UK) Limited pp. 337.

[DOR: 20.1001.1.16807073.2006.8.1.6.4]

3. Bowles, J. E., 1979. Physical and Geotechnical Properties of Soils. McGraw-Hill, Inc., England, 478 pp.
4. Casagli, N., and Rinaldi, M., 1995. Meccanismi di Instabilita Delle Sponde Nell'alveo del Fiume Sieve (Toscana). Quaderni di Geologia Applicata, **1:** 227-236.
5. Casagli, N., Rinaldi, M., Gargini, A., and Curini, A., 1999. Pore Water Pressure and Streambank Stability: Results from a Monitoring Site on the Sieve River, Italy. Earth Surf. Process. *Landforms*, **24**: 1095-1114.
6. Darby, S. E., and Simon, A. 1999. "*Incised River Channels*", John Wiley and Sons, Inc., England, 442pp.
7. Darby, S. E., and Thorne, C. R., 1994. Prediction of Tension Crack Location and Riverbank Erosion Hazards along Destabilized Channels. *Earth Surface Processes and Landforms*, **19**: 233-245.
8. Darby, S. E., and Thorne, C. R., 1996a. Modelling the Sensitivity of Channel Adjustments in Destabilized Sand-bed Rivers. *Earth Surface Processes and Landforms*, **21**: 1109-1125.
9. Darby, S. E., and Thorne, C. R., 1996b. Development and Testing of Riverbank-stability Analysis. *J. Hydr. Engrg., ASCE*, **122(8):** 443-445.
10. Darby, S. E., and Thorne, C. R., 1997. Discussion of "Development and testing of riverbank stability analysis" by Stephen Darby and Colin Thorne: Closure. *J. Hydr. Engrg., ASCE*, **123(11)**: 1052-1053.
11. Douglas, J. F., Gasiorek, J. M., and Swaffield, J. A., 1995. "*Fluid Mechanics*", Longman Singapore Publishers (Pte) Ltd., Singapore, 911pp.
12. Fredlund, D. G., Morgenstern, N. R., and Widger, R. A., 1978. The Shear Strength of Unsaturated Soils. *Canadian Geotechnical Journal*, **15(3)**: 312-321.
13. Fredlund, D., and Rahardjo, H., 1993. Soil Mechanics for Unsaturated Soils. Wiley and Sons, Inc., New York, 482 pp.
14. Hagerty, D. J., Spoor, M. F., and Parola, A.C., 1995. Near-bank Impacts of River Stage Control. *J. Hydr. Engrg., ASCE*, **121 (2)**: 196 -207.
15. Hillel, D., 1971. "*Soil and Water: Physical Principles and Processes*". Academic Press, Inc., New York.
16. Hoek, E., and Bray, J.W., 1981. Rock Slope Engineering Revised 3rd end, Institution of Mining and Metallurgy, London.
17. Huang, Y. H., 1983. "*Stability Analysis of Earth Slopes*" Van Nostrand Reinhold, New York, N. Y., 305pp.
18. Lawler, D. M., 1986. River Bank Erosion and the Influence of Frost: a Statistical Examination. Transactions of the Institute of British Geographers, **11**: 227-242.
19. Lohnes, R. A., 1991. A Method for Estimating Land Loss Associated with Stream Channel Degradation. *Engineering Geology*, **31**: 115-130.
20. Lohnes, R. A., and Handy, R. L., 1968. Slope Angles in Friable Loess. *Geology*, **76**: 247-258.
21. Millar, R. G., and Quick, M. C., 1997. Discussion of "Development and testing of riverbank stability analysis" by Stephen Darby and Colin Thorne. *J. Hydr. Engrg., ASCE*, **123(11)**: 1051.
22. Osman, A. M., and Thorne, C. R., 1988. Riverbank Stability Analysis. I: Theory. *J. Hydr. Engrg., ASCE*, **114(2)**:134-150.
23. Rinaldi, M., and Casagli, N., 1999. Stability of Streambanks Formed in Partially Saturated Soils and Effects of Negative Pore Water Pressure: the Sieve River (Italy). *Geomorphology*, **26**: 253-277.
24. Simon, A., Curini, A., Darby, S. E. and Langendoen, E. J., 2000. Bank and Near-bank Processes in an Incised Channel. *Geomorphology*, **35**: 193-218.
25. Simon, A., Darby, S. E., 1999. The Nature and Significance of Incised River Channels. In: "*Processes, Form, Engineering and Management*". (Eds.) Darby, S. E. and Simon, A., John Wiley and Sons, Inc., Chichester, U.K., PP. 3-18.
26. Simons, D. B., and Li, R. M., 1982. Bank Erosion on Regulated Rivers. In: "*Gravel-bed Rivers*" (Eds.): Hey, R. D., Bathurst, J. C. and Thorne, C. R., John Wiley and Sons, Inc., Chichester, U.K., PP. 717-274.
27. Simon, A., Wolfe, W. J., and Molinas, A., 1991. Mass Wasting Algorithms in an Alluvial Channel Model. Proceedings of the 5th Federal Interagency Sedimentation Conference, Las Vegas, Nevada, Vol. 2, p.8-22 to 8-29.
28. Spangler, M. G., and Handy, R. L., 1982. Soil Engineering, 4th Ed., Intext Educational, New York, N. Y., 819pp.
29. Taylor, D. W., 1948. "*Fundamentals of Soil Mechanics*", John Wiley and Sons, Inc., New York, N.Y.

[DOR: 20.1001.1.16807073.2006.8.1.6.4]

30. Terzaghi, K., and Peck, R. B. (1967). "*Soil Mechanics and Engineering Practice*", John Wiley and Sons, Inc., New York, N.Y., 729.
31. Thorne, C. R., 1982. Processes and Mechanisms of River Bank Erosion. In: "*Gravel-bed Rivers*", (Eds.): Hey, R. D., Bathurst, J. C. and Thorne, C. R., John Wiley and Sons, Inc., Chichester, U.K., PP. 227-271.
32. Thorne, C. R., 1990. Effects of Vegetation on Riverbank Erosion and Stability. In: "*Vegetation and Eosion*", (Ed.): Thorne, C. R., John Wiley and Sons, Inc., Chichester, U.K., PP. 125-144.
33. Thorne, C. R., and Abt, S. R., 1993. Analysis of Riverbanks Instability due to toe Scour and Lateral Erosion. *Earth Surface Processes and Landforms*, **18**: 835-843.
34. Thorne, C. R., Murphey, J. B., and Little, W. C., 1981. Stream Channel Stability Appendix D: Bank Stability and Bank Material Properties in the Bluffline streams of Northwest Mississippi. Report to U. S. Army Corps of Engineers, Vicksburg District, Vicksburg, Mississippi.
35. US Army Corps of Engineers, 1983. Sacramento River and Tributaries Bank Protection and Erosion Control Investigation. California Sediment Studies, Sacramento District, US Army Corps of Engineers.

مدل تحلیل پایداری ساحل رودخانه با لایه های چند گانه

ا. امیری تکلدانی و ا. دارابی

چکیده

فرسایش ساحل میتواند موجب از بین رفتن اراضی ساحلی به میزان قابل ملاحظه و در پی آن انتقال حجم زیادی از رسوبات به بازه های پایین دست رودخانه شود. در نتیجه توانایی پیش بینی پایداری و شکل هندسی سواحل تخریب یافته رودخانه یک پیش نیاز مهم برای تخمین میزان فرسایش ساحل و آورد رسوبی مربوطه میباشد. دراین مقاله یک مدل جدید به منظور تحلیل پایداری سواحل رودخانه هایی که از یک یا چند لایه از مصالح مختلف تشکیل شده اند ارایه شده است. در مدل جدید اثرات فشار مثبت آب منفذی در ناحیه اشباع و فشار منفی در ناحیه غیر اشباع ساحل رودخانه در نظر گرفته شده است. همچنین نقش فشار هیدرواستاتیکی ناشی از ارتفاع آب موجود در رودخانه در این مدل اعمال شده است. متفاوت با برخی از تحلیل های قبلی در رابطه با پایداری سواحل، در این مدل سطح خرابی به عبور از پنجه ساحل و نیز نیمرخ هندسی ساحل رودخانه به یک حالت خاص محدود نشده‌اند. مدل جدید با استفاده از اطلاعات موجود از دو منطقه مطالعاتی واقع در ایتالیا و آمریکا مورد آزمایش قرار گرفت. نتایج حاصله بیانگر تطابق میان مقادیر پیش بینی شده و مشاهده شده از پایداری ساحل در دو منطقه فوق میباشد.

[DOR: 20.1001.1.16807073.2006.8.1.6.4]